Cyclic peptide-polymer nanotubes as efficient and highly potent drug delivery systems for organometallic anticancer complexes

Sophie C. Larnaudie,[a] Johannes C. Brendel,[ǂa,b] Isolda Romero-Canelón,[a] Carlos Sanchez-Cano,[a] Sylvain Catrouillet,[c] Joaquin Sanchis,[b] James P. C. Coverdale,[a] Ji-Inn Song,[a] Abraha Habtemariam,[a] Peter J. Sadler,[a] Katrina A. Jolliffe,*[d] and Sébastien Perrier*[a,b,e]

[a] Department of Chemistry, University of Warwick, Gibbet Hill Road, Coventry CV4 7AL, United Kingdom.

[b] Faculty of Pharmacy and Pharmaceutical Sciences, Monash University, 381 Royal Parade, Parkville, VIC 3052, Australia.

[c] Institut Charles Gerhardt Montpellier, Place E Bataillon CC1702, 34095 Montpellier cedex 05, France

[d] The University of Sydney, School of Chemistry, Building F11, Sydney NSW 2006, Australia.

[e] Warwick Medical School, University of Warwick, Gibbet Hill Road, Coventry CV4 7AL, U.K.

ǂ Current address: Jena Center for Soft Matter (JCSM), Friedrich-Schiller-University, Philosophenweg 7, 7743 Jena, Germany.

*s.perrier@warwick.ac.uk; kate.jolliffe@sydney.edu.au

Abstract

Functional drug carrier systems have potential for increasing solubility and potency of drugs while reducing side effects. Complex polymeric materials, particularly anisotropic structures, are especially attractive due to their long circulation times. Here, we have conjugated cyclic peptides to the biocompatible polymer poly(2-hydroxypropyl methacrylamide) (pHPMA). The resulting conjugates were functionalised with organoiridium anticancer complexes. Small angle neutron scattering and static light scattering confirmed their self-assembly and elongated cylindrical shape. Drug-loaded nanotubes exhibited more potent antiproliferative activity towards human cancer cells than either free drug or the drug-loaded polymers, whilst the nanotubes themselves were non-toxic. Cellular accumulation studies revealed that the increased potency of the conjugate appears to be related to a more efficient mode of action rather than a higher cellular accumulation of iridium.

Keywords

Cyclic peptide, polymer nanotubes, self-assembly, organoiridium complexes, drug delivery.

Introduction

Advances in the development of small molecules as highly potent anticancer drugs often face limitations related to their poor solubility, rapid elimination and limited stability in the body.[1-2] The use of drug carriers may address these challenges by providing a protective shell that enhances solubility and retards clearance from the blood stream. Moreover, drug delivery vectors possess additional means of introducing functionality and increasing the selective accumulation at the specific target.[3] Tuneable in size, the devices can be optimized for passive targeting to tumours via the enhanced permeability and retention (EPR) effect.[4] In addition, most carriers can be functionalized by a variety of ligands (carbohydrates, peptides, proteins, antibodies, aptamers) to allow for active targeting of specific cells.[5] Overall, drug carrier systems offer potential for improving the therapeutic efficiency of drugs and reducing their side effects.

It is therefore not surprising that a plethora of potential drug delivery vectors has been reported including, for example, spherical polymer micelles or vesicles.[6] So-far-neglected, but particularly interesting, are organic nanotubes (NTs) formed by cyclic peptide-polymer conjugates. The nanotubes are built around a core made of β-sheet-forming cyclic peptides (CPs).[7] CPs presenting an even number of alternating D- and L- amino acids adopt a flat conformation in which the alignment of amide functionalities allows for the formation of hydrogen bonds between cyclic peptides, promoting their stacking into rod-like, cylindrical assemblies.[8] Cylindrical objects have been shown to exhibit a longer time of residence in the body than spheres of comparable size,[9] and rod-like structures can show higher activity than spherical particles[10] when loaded for example with active peptides,[11] antibodies[12] or proteins.[13] The high aspect ratio and the functionality of these organic nanotubes are potentially valuable design features for drug delivery.

Despite all the above mentioned advantages of these cyclic peptide nanotubes and the advances in the synthesis of functional materials, so far only a handful of examples of their use as drug delivery

vectors has been reported.[14-16] Blunden *et al.* have described the synthesis of such nanotubes bearing RAPTA-C, a moderately active ruthenium anticancer drug. They demonstrated that the attachment of the drug helped to increase its activity against cancer cells.[14]

Here, we present a specifically designed system comprising a self-assembling CP core, a functional polymer shell and a highly potent organoiridium candidate drug. Particular attention was paid to the use of biocompatible components in the synthesis and the effective attachment of the metallodrug through efficient drug conjugation suitable for cancer therapy. In this context, poly(2-hydroxypropyl methacrylamide) (pHPMA) was chosen, since it has attracted particular interest for drug delivery applications over the past few decades.[17-18] Several systems derived from pHPMA have been studied in detail and are currently undergoing clinical trial.[19-20]

In addition to comprehensive optimisation of the delivery vector, the choice of a compatible and potent drug is critical for designing effective therapeutics. Recently, organoiridium catalysts have been shown to exhibit high potency towards a wide range of cancer cells[21] and through careful choice of ligands, the efficiency of these complexes can be improved by three orders of magnitude, reaching sub-micromolar values.[22] Depending on the cell line and the complex, activity was shown to be *ca.* 5 to 10 times higher than that of the clinical drug cisplatin, and more than 200 times higher than RAPTA-C. The attachment of this type of complex to a polymeric carrier can be achieved through incorporation of a suitable metal-binding ligand on the polymer chains.

Based on these considerations, we synthesized a cyclic peptide-pHPMA conjugate and loaded it with an organoiridium anticancer complex. The organoiridium fragment was attached through ligation to a pyridine-containing comonomer in the polymer shell. The ability of the drug-loaded conjugates to self-assemble into nanotubes in solution was thoroughly established by scattering techniques, and their cytotoxicity *in vitro* was assessed and compared to that of the free drug. For the first time, it was also tested alongside and a drug-loaded polymer control that does not contain the cyclic peptide core, in order to clearly assess the impact of the self-assembly on the cytotoxicity. Finally, cellular

accumulation of the three compounds was studied both qualitatively and quantitatively and the mechanism of action was explored.

Experimental section

Materials

4-Aminomethyl pyridine (98%), 1-amino-2-propanol (95%), methacryloyl chloride (97%), and deuterated solvents for NMR were purchased from Sigma-Aldrich. *N*-methylmorpholine (NMM, 99 %) was purchased from Alfa Aesar. Potassium carbonate and anhydrous magnesium sulfate ($MgSO_4$) were purchased from Fisher Scientific. 2,2'-Azobis[2-(2-imidazolin-2-yl)propane]dihydrochloride (VA-044) was purchased from Wako Chemicals. *O*-(Benzotriazole-1-yl)-*N,N,N',N'*-tetramethyluronium hexafluorophosphate (HBTU) was purchased from Iris Biotech. All solvents were bought from commercial sources and used as received. The cyclic peptide and the chain transfer agents CPAETC and $E(CPAETC)_2$ were synthesized according to previously reported protocols.[23-24] [(Cp*)-Ir-(phpy)(Cl)] and [(Cp^{xph})-Ir(phpy)(Cl)] were synthesized and characterized as previously described.[25-26]

Characterization methods

NMR spectra were recorded on a Bruker DPX-300 instrument. Mass spectra were obtained on an Agilent 6130B Single Quad. Molecular weights and dispersities of the polymers were assessed by size exclusion chromatography (SEC) on a Polymer Laboratories PL-GPC 50 Plus system in DMF with 0.1% LiBr, using a poly(methyl methacrylate) calibration. Infrared absorption experiments were performed on a Bruker VECTOR-22 FTIR spectrometer. The incremental refractive index, d*n*/d*C*, was determined by measuring the refractive index of the polymer in water at various concentrations ranging from 0.25 to 2 mg/mL, using a Shodex RI detector operating at a wavelength of 632 nm.

SANS was carried out on the Sans2d small angle diffractometer at the ISIS Pulsed Neutron Source (STFC Rutherford Appleton Laboratory, Didcot, UK).[27-28] A collimation length of 4 m and incident wavelength range of 1.75 – 16.5 Å was employed. Data were measured simultaneously on two 1 m^2 detectors to give a *q*-range of 0.0045 – 1.00 $Å^{-1}$. The small-angle detector was positioned 4 m from

the sample and offset vertically 60 mm and sideways 100 mm. The wide-angle detector was positioned 2.4 m from the sample, offset sideways by 980 mm and rotated to face the sample. The wave vector, q, is defined as:

$$q = \frac{4\pi \sin\frac{\theta}{2}}{\lambda} \quad (1)$$

where θ is the scattered angle and λ is the incident neutron wavelength. The beam diameter was 8 mm. Samples were prepared at a concentration of 5 mg/mL in deuterated phosphate buffer saline (PBS), and were contained in 2 mm path length quartz cells. Each raw scattering dataset was corrected for the detectors efficiencies, sample transmission and background scattering and converted to scattering cross-section data ($\partial\Sigma/\partial\Omega$ *vs.* q) using the instrument software.[29] These data were placed on an absolute scale (cm^{-1}) using the scattering from a standard sample (a solid blend of hydrogenous and perdeuterated polystyrene) in accordance with established procedures.[30]

Light scattering measurements were obtained using an ALV-CGS3 system operating with a vertically polarized laser with a wavelength of 632 nm. The measurements were taken at 20°C over a range of scattering wave vectors.

Synthetic procedures

Synthesis of 2-hydroxypropyl methacrylamide (HPMA)

Potassium carbonate (29 g, 1.1 eq., 0.21 mol) was dispersed in 120 mL of dry DCM. The mixture was cooled to -10°C with an ice-ethanol bath and 1-amino-2-propanol (14.5 mL, 1 eq., 0.19 mol) was added. Methacryloyl chloride (18.5 mL, 1 eq., 0.91 mol) was diluted with 20 mL of dry DCM, and added dropwise to the previous mixture, while maintaining the temperature at -10°C. Once the addition was complete, the reaction was left to warm up to room temperature and stirred overnight. After filtration and drying over $MgSO_4$, the DCM was evaporated and a white solid was obtained. The product was dissolved in methanol and washed with hexane, and the methanol phase was evaporated. The obtained solid was recrystallized from acetone. Yield: 45% (10.2 g). ^{1}H-NMR (d_6-DMSO, 300 MHz, ppm): δ = 7.82 (broad s, 1H, N*H*) , 5.65 (s, 1H, C*H* vinyl), 5.31 (s, 1H, C*H* vinyl), 4.71 (s, 1H,

O*H*), 3.69 (m, 1H, C*H*), 3.05 (m, 2H, CH_2), 1.85 (s, 3H, CH_2=C(CH_3)), 1.00 (d, *J* = 6 Hz, 3H, CH-CH_3). ^{13}C-DEPT-NMR (d_6-DMSO, 75 MHz, ppm): δ = 167.7, 139.9, 118.9, 85.1, 46.7, 21.1, 18.6.

Synthesis of 2-(3-(pyridin-4-ylmethyl)ureido)ethyl)methacrylate (PUEMA)

2-Isocyanatoethyl methacrylate (2.2 g, 14.15 mmol) and 4-aminomethyl pyridine (1.53 g, 1 eq., 14.15 mmol) were mixed in dry DCM (10 mL) and left to stir at room temperature for 10 min. The solvent was evaporated under reduced pressure and PUEMA was collected as a white powder. Yield: 95% (3.53 g). ^{1}H-NMR ($CDCl_3$, 300 MHz, ppm): δ = 8.52 (d, 2H, C*H*-N-C*H* pyridine), 7.19 (d, 2H, C*H*-C-C*H* pyridine), 6.09 (s, 1H, C*H* vinyl), 5.59 (s, 1H, C*H* vinyl), 5.13 (broad t, 1H, N*H* urea), 4.97 (broad t, 1H, N*H* urea), 4.38 (d, 2H, NH-CH_2-pyridine), 4.25 (t, 2H, O-CH_2), 3.53 (q, 2H, O-CH_2-CH_2), 1.93 (s, 3H, CH_3). ^{13}C-DEPT-NMR ($CDCl_3$, 75 MHz, ppm): 166.9, 157.5, 149.2, 148.3, 135.3, 125.5, 121.4, 63.4, 42.4, 39.0, 17.6. FTIR: (ν, cm^{-1}): 3313 (N-H stretch, urea), 1720 (C=O stretch, methacrylate), 1623 (C=C stretch, alkene), 1585 (C=O stretch, urea). MS (ESI): $[M+Na]^+$ calculated: 286.1, found: 285.9.

Copolymerization of HPMA and PUEMA

Chain transfer agent (CTA), monomers, initiator (VA 044) and solvent (30 % water in DMSO) were introduced into a flask equipped with a magnetic stirrer and sealed with a rubber septum. (See Table S1 for detailed conditions). The solution was degassed by bubbling nitrogen through it for 15 min, and then put in an oil bath at 44°C for 24 h in the case of kinetics experiments. Subsequent polymerizations were stopped after 18 h, when the conversion of PUEMA and HPMA reached > 99% and 75%, respectively. The polymers were precipitated in ice-cold acetone and dried under vacuum.

Conjugation of polymers to CP

The cyclic peptide, p$HPMA_{51}$-*co*-$PUEMA_{3.5}$ (2.5 eq.) and HBTU (3.75 eq.) were solubilized in DMSO (1.5 mL). NMM (6 eq.) was added to the reaction mixture and it was left to stir at room temperature for 2 h. After the reaction, DMSO was removed using a stream of N_2 and the conjugates

were dissolved in water and purified from the excess polymer using a centrifugal ultrafiltration unit with a molecular weight cut off of 30 kDa (Amicon® Ultra centrifugal filter). The isolated conjugates were freeze-dried.

Complexation of the iridium complexes to the conjugates

[(Cp*)-Ir-(phpy)(Cl)] (15.6 mg, $3.02.10^{-5}$ mol) was dissolved in water/methanol 1/1 (12 mL) in a vial wrapped in aluminium foil, and silver nitrate (5.12 mg, 1 eq., $3.02.10^{-5}$ mol) was added. The mixture was stirred at room temperature overnight, and centrifuged to remove the silver chloride salts. The supernatant was decanted in a round bottomed flask and CP-(p(HPMA$_{51}$-*co*-PUEMA$_{3.5}$))$_2$ (25.7 mg, 3 mol eq. of Ir per pyridine unit, $1.44.10^{-6}$ mol) was added. The reaction was left to stir for 2 days, after which most of the solvent was evaporated, keeping ~ 1 mL. The drug-loaded conjugates were purified from the excess complex on a disposable size exclusion column (PD10, Sephadex G25, GE Healthcare) and freeze dried. The drug loading was determined by ^{1}H-NMR in MeOD. The same protocol was used for the complexation of [(Cp*)-Ir-(phpy)(Cl)] to pHPMA$_{93}$-*co*-PUEMA$_7$ and of [(Cp^{xph})-Ir-(phpy)(Cl)] to CP-(p(HPMA$_{51}$-*co*-PUEMA$_{3.5}$))$_2$ and pHPMA$_{93}$-*co*-PUEMA$_7$.

Inductively coupled plasma (ICP)

Measurements of trace Ir in biological samples were determined using ICP techniques. Ir standard solution (iridium chloride, 995 ± 4 µg/mL in 10% v/v hydrochloric acid) was purchased from Inorganic Ventures. Ultra-pure nitric acid (72%) was freshly distilled and diluted using milliQ water to achieve 3.6% v/v working concentration.

For iridium-containing solutions in culture medium, iridium concentration was determined using a Perkin Elmer Optima 5300 DV Optical Emission Spectrophotometer (ICP-OES) with standard addition of sodium chloride (TraceSELECT) to freshly prepared calibration standards (50-700 ppb) to match the sample matrix. Data were processed using WinLab32 V3.4.1 for Windows (Perkin Elmer).

For cell digest samples, iridium concentration (ng × 10^6 cells) was determined using a Agilent Technologies 7500 series ICP-MS in no-gas and He-gas mode. Calibration standards for ^{193}Ir were

freshly prepared (0.1-1000 ppb) and an internal standard (^{167}Er, 50 ppb) was used. Data were processed using ChemStation version B.03.05 (Agilent Technologies, Inc.).

In vitro **testing**

Cell Culture

Human A2780 ovarian carcinoma cells were obtained from the European Collection of Cell Cultures (ECACC) used between passages 5 and 18 and were grown in Roswell Park Memorial Institute medium (RPMI-1640) or Dulbecco's Modified Eagle's Medium (DMEM) supplemented with 10% v/v of foetal calf serum, 1% v/v of 2 mM glutamine and 1% v/v penicillin/streptomycin. HOF human ovarian fibroblasts were obtained from ScienCell Research Laboratories, and maintained in fibroblast medium supplemented with 2% v/v of foetal calf serum, 1% v/v of penicillin/streptomycin and 1% v/v of growth factor serum. They were grown as adherent monolayers at 37°C in a 5% CO_2 humidified atmosphere and passaged at approximately 70-80% confluence.

Growth Inhibition Assay

Briefly, 5000 cells were seeded per well in 96-well plates. The cells were pre-incubated in the corresponding drug-free media at 37°C for 48 h before adding different concentrations of the compounds to be tested. Stock solutions of the Ir(III) complexes themselves were firstly prepared in 5% v/v DMSO and 95% v/v either PBS or cell culture medium, for the 'conjugated complexes' or polymer/conjugate controls the use of DMSO was omitted. The concentration of Ir solutions was determined by ICP-OES before drug administration. In all cases, stock solutions were further diluted in cell culture medium until working concentrations were achieved, maintaining the total amount of DMSO below 1%. The drug exposure period was 24 h. After this, supernatants were removed by suction and each well was washed with PBS. A further 72 h was allowed for the cells to recover in drug-free medium at 37°C. The SRB assay was used to determine cell viability. Absorbance measurements of the solubilised dye (on a BioRad iMark microplate reader using a 470 nm filter) allowed the determination of viable treated cells compared to untreated controls. IC_{50} values (concentrations which caused 50% of cell growth inhibition), were determined as duplicates of

triplicates in two independent sets of experiments and their standard deviations were calculated. Two-tailed t-tests were performed assuming equal variance.

Equipotent metal accumulation in cancer cells

Cell accumulation studies of Iridium complexes were conducted on A2780 ovarian cells. Briefly, 3 x 10^6 cells were seeded on a Petri dish. After 24 h of pre-incubation time in drug-free medium at 37°C, the compounds were added to give final concentrations equal to IC_{50} (the concentration of Ir solutions was determined by ICP-OES before drug administration) and 24 h of drug exposure were allowed. After this time, cells were washed, treated with trypsin, counted, and cell pellets were collected. Each sample was digested in Wheaton v-vials using 200 µL of 72% v/v nitric acid at 80°C overnight (72%) and then diluted with milliQ water to achieve final concentration of 3.6% v/v acid. ^{193}Ir concentration was determined by ICP-MS in both no-gas and He-gas mode. These experiments were all carried out in triplicate and the standard deviations were calculated.

Equimolar metal accumulation in cancer cells

Experiments were carried out as described above with the following modifications: drug concentrations were equimolar and equal to 0.60 µM. Drug exposure times were kept unchanged (24 h).

Time-dependent metal accumulation in cancer cells

Experiments were carried out as described above with the following modifications: drug exposure times were: 1 h, 2 h, 4 h, 6 h, 14 h and 24 h at equipotent concentrations equal to IC_{50} values.

Metal accumulation in cancer cells at 4°C

Experiments were carried out as described above with the following modifications: plates were placed at 4°C 20 min prior to dosing at IC_{50} values, and drug exposure was limited to 4 h.

Cellular metal distribution

Cell pellets were obtained as described above, and were fractionated using the FractionPREP kit from BioVision according to the supplier's instructions. Each sample was digested in Wheaton v-vials using 200 µL of 72% v/v nitric acid at 80°C overnight (72%) and then diluted with milliQ water to achieve final concentration of 3.6% v/v acid. ^{193}Ir concentration was determined by ICP-MS in both no-gas and He-gas mode. These experiments were all carried out in triplicate and the standard deviations were calculated.

Results and discussion

Synthesis of the polymer and conjugate carriers

The well-studied monomer building block 2-hydroxypropyl methacrylamide (HPMA) was chosen as the main monomer for designing the polymeric drug used in this work. In order to provide a binding site for the ligation of anticancer iridium complexes, a comonomer was introduced. Pyridine was chosen as the binding ligand, since it can readily replace the chloride ligand present on the selected organoiridium precursor. Moreover, organoiridium pyridine complexes themselves exhibit good anticancer activity (0.1-10 µM depending on the cell line and the nature of the other ligands).[22, 31] 2-(3-(Pyridin-4-ylmethyl)ureido)ethyl)methacrylate (PUEMA) was therefore synthesized and characterized (see Supporting Information, Figures S3-5).

The cyclic peptide-polymer conjugate **2** containing pHPMA-*co*-PUEMA was synthesised using Reversible Addition Fragmentation Chain Transfer (RAFT) copolymerisation of HPMA with 5 % PUEMA, leading polymer **1**, followed by coupling of the polymer to the chosen cyclic peptide, cyclo(D-Leu-Lys-D-Leu-Trp)$_2$ (Scheme 1 and Table 1).[32-33]

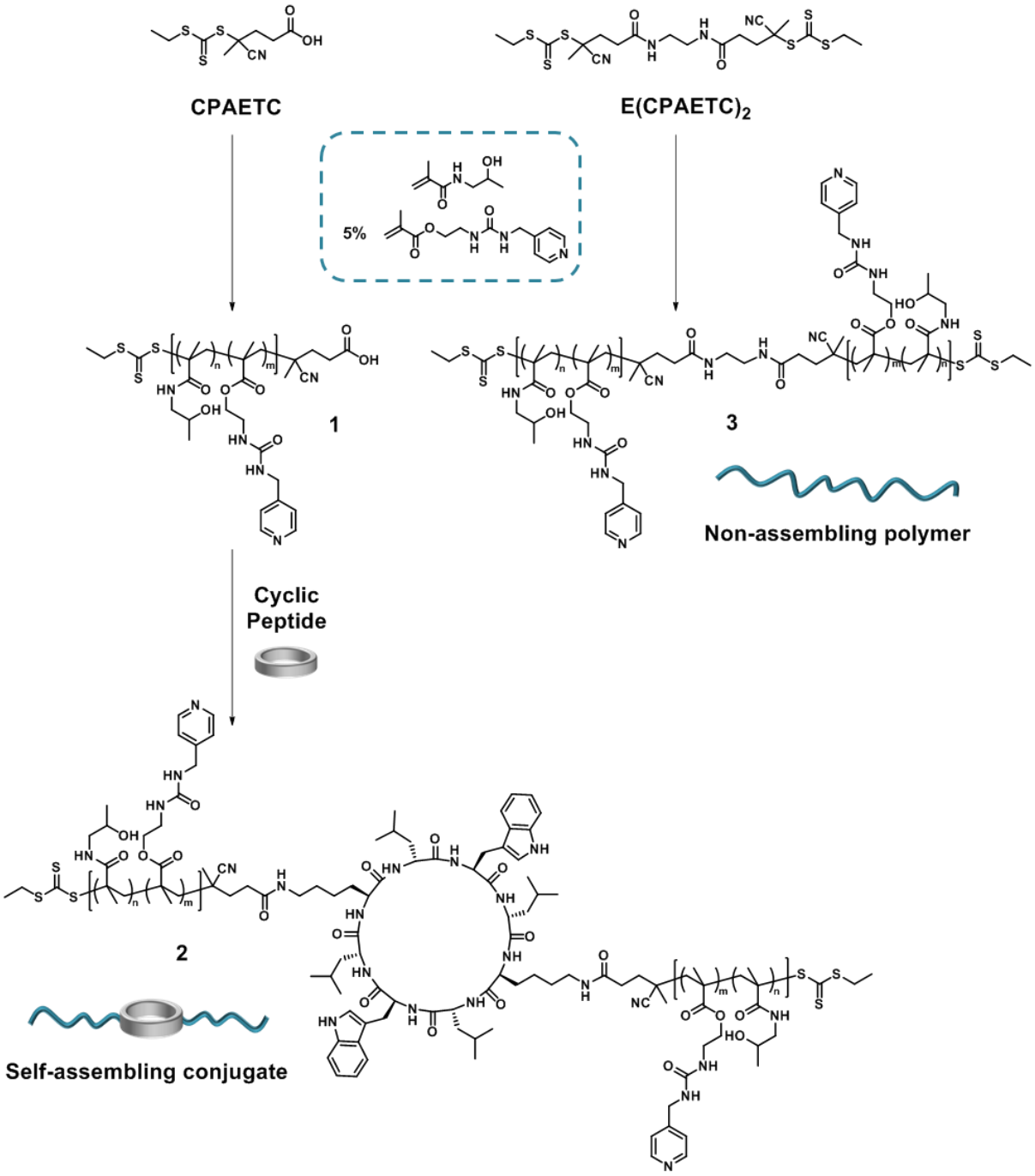

Scheme 1. Synthesis of materials.

Kinetic measurements of the copolymerization using (4-cyano pentanoic acid)yl ethyl trithiocarbonate (CPAETC) showed that PUEMA was consumed significantly faster than HPMA, indicating a higher reactivity (Figure S6). The direct consequence of this observation is that the functional monomer tends to be incorporated first, meaning that most of the pyridine ligands for metallodrug attachment will ultimately be located towards the α-chain end of polymer **1**. The bifunctional RAFT agent 1,2-

bis((4-cyano pentanoic acid)yl ethyl trithiocarbonate)-ethane diamide (E(CPAECTC)$_2$) was used to provide a non self-assembling polymeric control **3** to the peptide-polymer conjugate **2** (Scheme 1). The obtained polymers **1** and **3** were well defined, with narrow dispersities of 1.16 and 1.12, respectively (Table 1 and Figure S7). Using monomer conversions, the final content of PUEMA in polymer **1** and polymer **3** was estimated to be 6.5 and 7 %, respectively. These values were confirmed by ^{1}H NMR of the precipitated polymer (Figures S8-9).

Copolymer **1** was attached to the cyclic peptide by reacting the amine groups present on the cyclic peptide with the carboxylic acid end-group of **1**, using *O*-(benzotriazol-1-yl)-*N,N,N′,N′*-tetramethyluronium hexafluorophosphate (HBTU) as a coupling reagent. The coupling was complete after 1 h and the water-soluble nature of these conjugates enabled straightforward purification by dialysis. The purified conjugate **2** was well-defined, with a dispersity of 1.19 (Table 1 and Figure S10). Interestingly, since the attachment occurs at the *α*-chain end of the polymer, the pyridine units used for organoiridium attachment are located on average close to the cyclic peptide core, allowing the HPMA-richer shell to provide shielding of the drug from the environment.

Table 1. Summary of polymers used in this work.

Entry	Material	$M_{n,\,th}$[a] (g.mol^{-1})	$M_{n,\,GPC}$[b] (g.mol^{-1})	$Đ$[b]
1	p(HPMA$_{51}$-*co*-PUEMA$_{3.5}$)	8400	14 800	1.16
2	CP-(p(HPMA$_{51}$-*co*-PUEMA$_{3.5}$))$_2$	17800	29200	1.19
3	pHPMA$_{93}$-*co*-PUEMA$_7$	15700	21400	1.12

[a] Determined by ^{1}H NMR. [b] Determined by SEC using DMF (0.1% LiBr) as eluent, calibrated with pMMA standards.

Complexation of organoiridium anticancer drugs

The attachment of the selected iridium complexes to the polymer **3** and cyclic peptide-polymer conjugate **2** was achieved following a ligand exchange procedure previously used to synthesize pyridine analogues of the chloride-containing drugs.[31] The chloride ligand of the iridium complexes **4a** and **4b** was first removed using silver nitrate, followed by complexation to the pyridine units of the polymer chains (Scheme 2). The complexes used in this work were the [(Cp*)Ir(phpy)Cl] (abbreviated as Ir-Cp*, **4a**), which contains pentamethylcyclopentadienyl (Cp*) and *C,N*-chelated

phenylpyridine (phpy) as ligands,[26] as well as the more hydrophobic [(Cp^{xph})Ir(phpy)Cl] (Ir-Cp^{xph}, **4b**), in which the Cp* is replaced by an extended phenyltetramethylcyclopentadienyl (Cp^{xph}) ligand.[25]

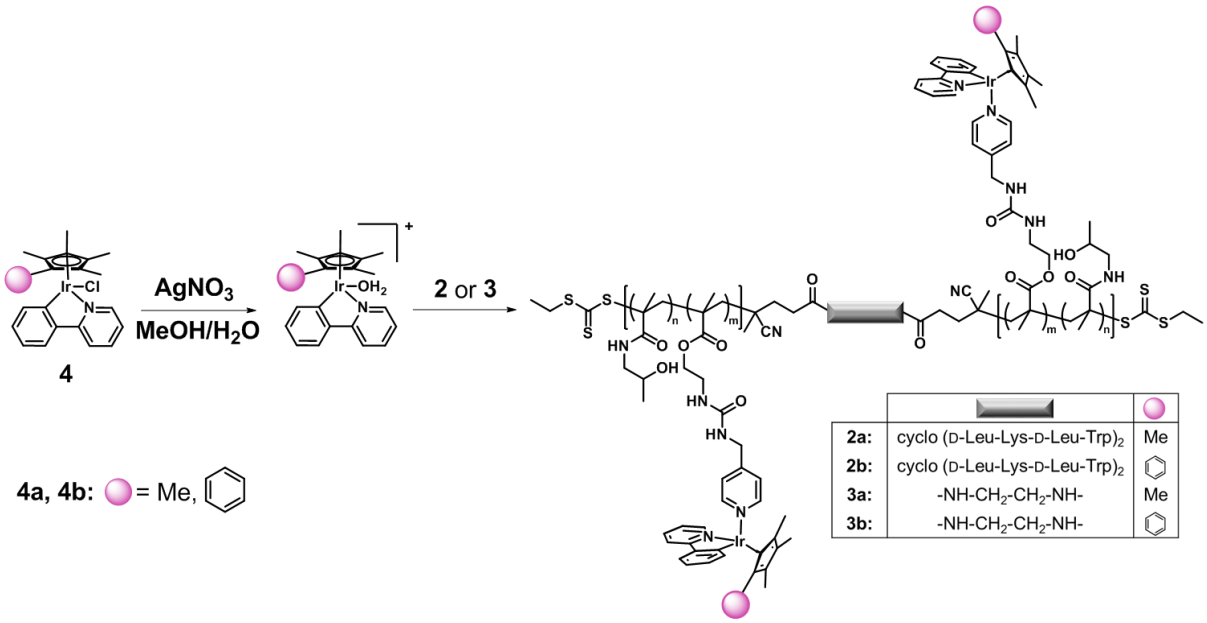

Scheme 2. Synthesis of drug-loaded compounds: complexation of organoiridium complexes **4a** and **4b** to conjugate **2** and polymer **3**.

An excess of the iridium complex **4** (3 mol equiv per pyridine site) was used to maximise the drug loading onto the polymer and peptide-polymer conjugate. After purification by size exclusion chromatography, the drug-bearing compounds (conjugates **2a** and **2b**, and polymers **3a** and **3b**) were characterized by ^{1}H NMR spectroscopy (Figure 1 and Figures S11-13). The shifts of characteristic peaks of the complex and of the pyridine units as well as the broadening of the signals associated with the complex clearly indicate full complexation of the drug to the polymer.

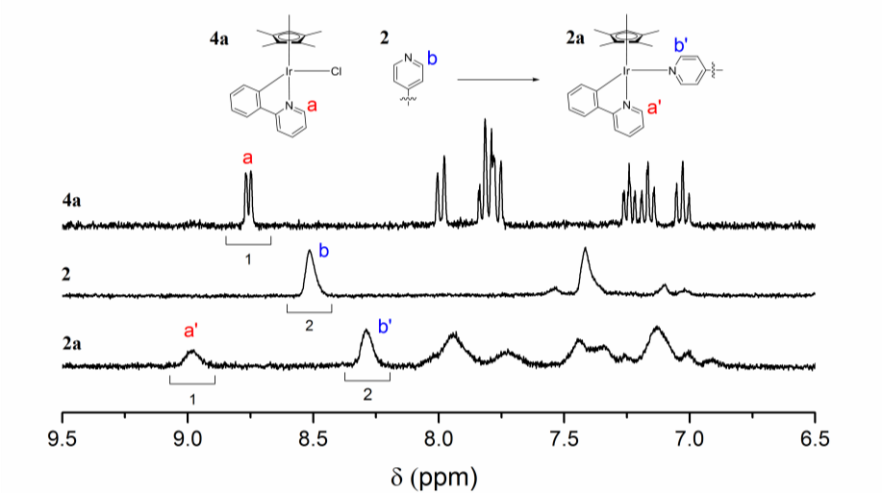

Figure 1. ^{1}H NMR characterization of the attachment of complex **4a** onto conjugate **2**, affording conjugate **2a.**

Characterization of supramolecular nanotubes

In order to confirm the self-assembly of the conjugates into tubular structures, the drug-bearing conjugate **2a** was dissolved in PBS and small angle neutron scattering (SANS) and static light scattering (SLS) measurements were performed (Figure 2).

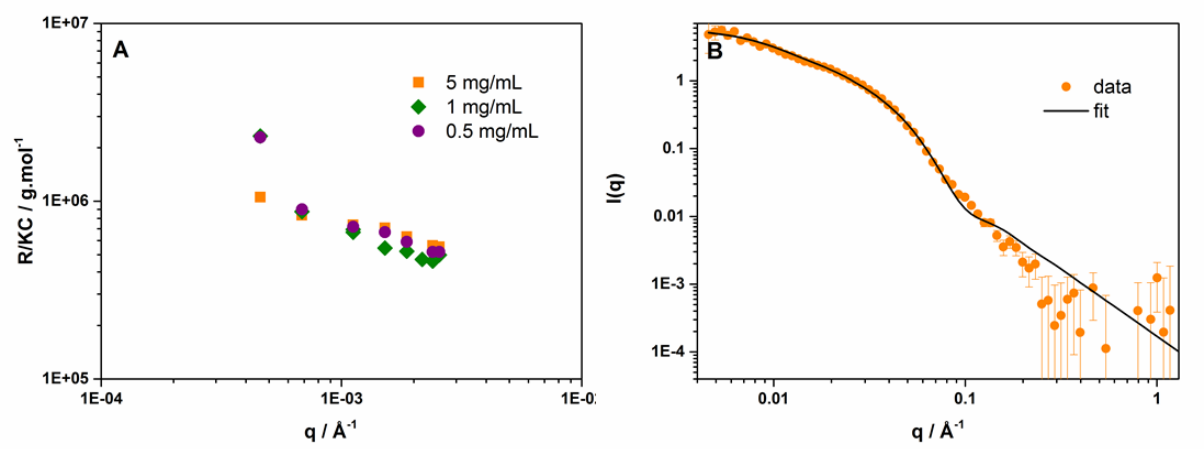

Figure 2. A) Static light scattering profile of conjugate **2a** in solution in PBS at different concentrations**.** B) Small angle neutron scattering profile of conjugate **2a** (orange dots) and its fit using a cylindrical micelle model (black line).

The SANS data were fitted with a cylindrical micelle model (Figure 2B), which accounts for both the overall elongated shape provided by the self-assembled cyclic peptide core (characteristic q^{-1} dependency at low q values: cylinder form factor) and the polymer arms (Gaussian chain form factor

at high q values).[34] By fitting geometrical parameters, reasonable values were obtained starting from a radius of 5 Å for the peptide core, in accordance with previously reported results (see Supporting Information, Table S2).[8, 35] However, the maximum length of these tubes cannot be fully determined by these SANS measurements, as the scattering intensity is still increasing at the lowest measured q values and does not show the formation of a plateau which is indicative of a limited length. Static light scattering (SLS) measurements were then carried out since this technique allows access to a larger window of observation (Figure 2A). SLS experiments showed that the molecular weight of the assemblies was not affected by the concentration of the solution (within the tested range) and this molecular weight was determined to be $9.74.10^5 \pm 0.37.10^5$ g.mol^{-1} for the drug-bearing conjugate. Using the molecular weight of the unimer and the previously reported distance between adjacent peptides,[7, 35] the average length of the objects can be determined as 21.8 ± 0.9 nm, corresponding to 46 assembled conjugates (see Supporting Information, Figure S14 and Table S3).

Anticancer activity and cellular accumulation

The antiproliferative activity of the polymers and conjugates was initially determined for A2780 human ovarian cancer cells, as IC_{50} values, the concentrations at which 50% of cell growth is inhibited (Figure 3).

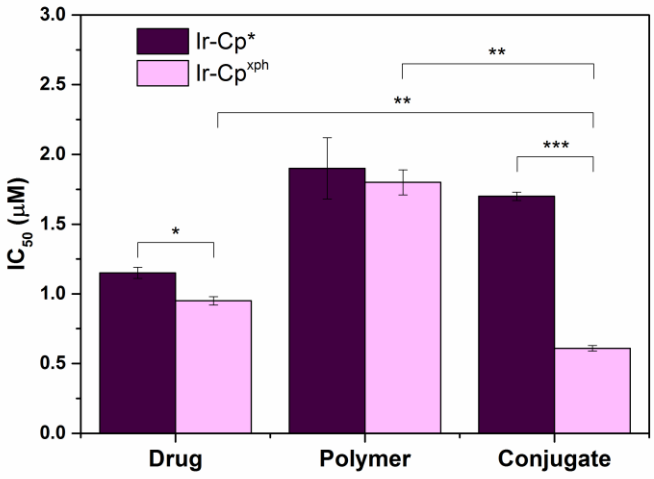

Figure 3. Antiproliferative activity in A2780 cells: IC_{50} values for free organoiridium complexes, drug-bearing polymers, and drug-bearing conjugates using Ir-Cp* (dark) and Ir-Cp^{xph} (light) as the drug. *p < 0.05, **p < 0.01, ***p < 0.001.

The drug-free control samples (polymer alone and cyclic peptide-polymer conjugates) were non-toxic in the tested range of concentrations (Figure S15). However, the organoiridium-containing samples showed high activity. For both drugs, the IC_{50} of the loaded polymers was slightly higher (however still in the same order of magnitude) than that of the free drug: 1.90 ± 0.22 μM for the polymer **3a** compared to 1.15 ± 0.04 μM for Ir-Cp*, and 1.80 ± 0.09 μM for the polymer **3b** compared to 0.95 ± 0.03 μM for Ir-Cp^{xph}. For Ir-Cp*, no major difference was observed between the polymer and the conjugate (1.90 ± 0.22 μM for the polymer **3a** compared to 1.70 ± 0.03 μM for the conjugate **2a**). However the IC_{50} of the conjugate **2b** (0.61 ± 0.02 μM) in A2780 was 3x lower than that of the drug-loaded polymer **3b** (1.8 ± 0.09 μM). This substantial increase in activity between the polymer and the nanotubes suggests that the self-assembly has a noticeable impact on the behaviour of the carrier. Furthermore, the conjugate **2b** was twice as potent as the free drug Ir-Cp^{xph}. For all the studied compounds the IC_{50} values were lower for Ir-Cp^{xph}, which is a more hydrophobic complex than for Ir-Cp*. This result shows the same trend as previously reported data for the complexes themselves[25-26] (the present values are slightly different due to the updated protocol involving confirmation of Ir concentrations by ICP-OES measurements). These organoiridium complexes have not been previously conjugated to delivery vectors, but it is clear from previous studies that increasing the hydrophobicity of the cyclopentadienyl ligand enhances their antiproliferative activity.[22, 25, 36] The present report suggests that this is also the case when the complexes are conjugated to polymers and cyclic peptide-polymer conjugates. For this reason, further studies focussed on the more potent compounds bearing Ir-Cp^{xph}.

The antiproliferative activity of the three compounds (Ir-Cp^{xph} as free drug, loaded onto the polymer (**3b**), and the conjugate (**2b**)) was then determined against human ovarian fibroblasts (HOF), a model for healthy, non-cancerous cells, and compared to that against A2780 ovarian cancer cells (Figure 4).

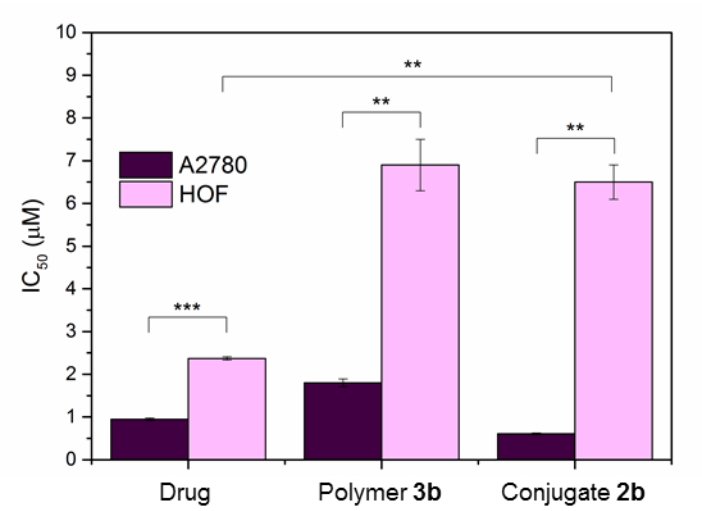

Figure 4. Antiproliferative activity of free drug Ir-Cp^{xph}, drug-bearing polymer **3b** and drug-bearing conjugate **2b** in A2780 (cancer, dark) and HOF (healthy, light) ovarian cells. **p < 0.01, ***p < 0.001.

All compounds were found less toxic in normal HOF cells than in A2780. The observed selectivity is likely attributable to the nature of the drug. This class of iridium anticancer complexes has previously been shown to exhibit selectivity towards cancer cells, which is believed to rely on interference with cellular redox homeostasis (the ability of the cells to regulate their levels of reactive oxygen species) in cancer cells specifically.[21]

The increased activity of the conjugate **2b** compared to the polymer **3b** and the free drug in A2780 cells may be related either to enhanced cellular accumulation or to a more efficient mode of action, for example through a different partitioning of the drug amongst the cell organelles. The possibility of enhanced accumulation (the balance of the uptake and efflux equilibrium), was investigated by exposing A2780 cells to the Ir-Cp^{xph} compounds (free drug, polymer and conjugate) at their respective IC_{50} values. At regular intervals over 24 h, cells were collected and digested in nitric acid to determine the amount of iridium accumulated using inductively coupled plasma mass spectrometry (ICP-MS) (Figure 5).

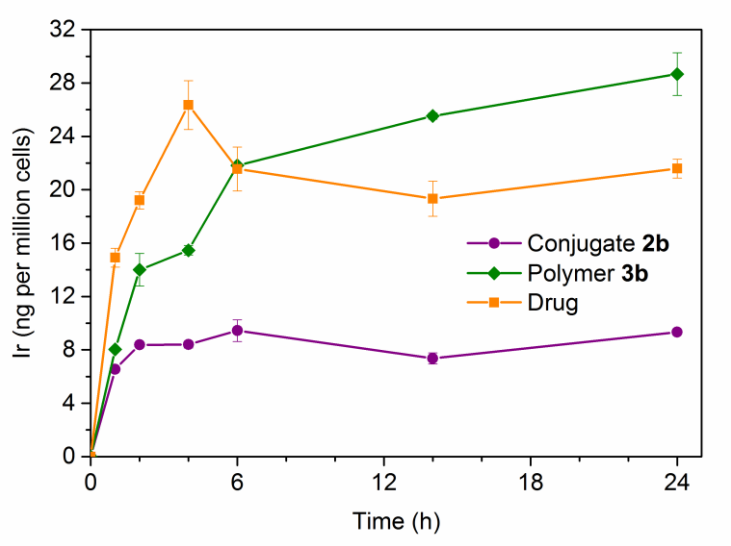

Figure 5. Iridium accumulated in A2780 cells after 24 h of exposure to the free drug Ir-Cp^{xph} (orange squares), the drug bearing polymer **3b** (green diamonds) and the drug bearing conjugate **2b** (purple circles) at equipotent IC_{50} conditions.

Figure 5 shows that the kinetics of uptake are different for the three compounds: the maximum amount of iridium accumulated is reached after only 2 h in the case of the conjugate **2b**, after which it remains the same, while for the polymer **3b**, the amount is still increasing after 24 h. In the case of the free drug, the amount of iridium peaks at 4 h, before decreasing slightly. Such cellular efflux is common for organometallic complexes.[37-38] These differences in the rate and profile of uptake suggest that the conjugate interacts differently with the cells. After 24 h of exposure to the free drug, the drug-bearing polymer and the drug-bearing conjugate under equipotent conditions, each at their IC_{50} concentrations (0.95 μM, 1.80 μM and 0.61 μM, respectively), 21.6 ± 0.7 ng, 28.7 ± 1.6 ng and 9.3 ± 0.2 ng of iridium per million cells were accumulated, respectively. Taking the differences of the IC_{50} values into account, similar percentages of the total amount of iridium administered are retained: 7.7 ± 0.2 % of the initial amount was accumulated for the drug, 6.5 ± 0.4 % for the polymer and 6.5 ± 0.1 % in the case of the conjugate. These values are similar to those observed previously for organometallic drugs.[31, 38]

The results suggest that the increased cytotoxicity of the conjugate **2b** compared to the other compounds is not due to enhanced uptake of iridium by the cells, and are further supported by the amount of iridium accumulated after exposure under equimolar conditions. The cells were incubated in the presence of the three compounds at the lowest IC_{50} (0.61 μM). Under these conditions, similar amounts of iridium were accumulated (10.1 ± 0.1 ng per million cells for the free drug, 10.5 ± 0.2 ng for the polymer and 9.3 ± 0.8 ng for the conjugate). We conclude that the attachment of the drug to the polymer or the conjugate does not affect the extent of the accumulation of iridium in the cells, which suggests that the nanotubes rather exhibit a more effective mode of action, for example through a different partitioning of the drug amongst the cell organelles.

In order to evaluate this partitioning, equipotent uptake experiments were repeated and the cell pellets collected after 24 h. The iridium content of the membrane, cytosol, cytoskeleton and nucleus fractions was determined by fractionation of the cell compartments, and the results are shown in Figure 6A. The total amount of iridium in each fraction follows the trend previously observed for whole cells: the amount of iridium increases in the order conjugate < drug < polymer. The percentage of iridium in the membrane fraction increases slightly in the order drug (56 %) < polymer (65 %) ≈ conjugate (69 %), which may indicate that the polymer-conjugated drugs favour an endocytosis-mediated pathway, since endosomes and lysosomes are collected in the membrane fraction. To confirm that the polymer and conjugate follow an energy-dependent mechanism, accumulation experiments were undertaken at 4°C, conditions known to block endocytosis processes (Figure 6B).[39] At 4°C the free drug accumulated to an extent of 3.8 ± 0.2 ng Ir per 10^6 cells, which corresponds to about 15% of the amount accumulated at 37°C, suggesting that energy-independent pathways (such as passive diffusion) play at least a partial role in the cellular accumulation of the free drug, in accordance with previous reports.[38] The polymer **3b** accumulated to a lesser extent, with 1.9 ± 0.3 ng Ir per 10^6 cells. In contrast the conjugate **2b** did not accumulate significantly in these conditions, supporting the hypothesis that cell entry involves energy-dependent mechanisms.

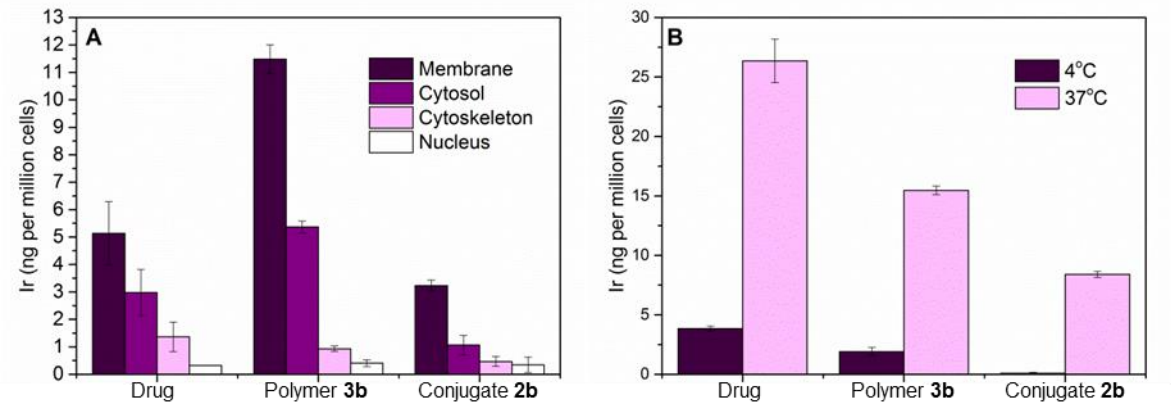

Figure 6. A) Iridium content of the membrane, cytosol, cytoskeleton and nucleus fractions of A2780 cells after 24 h of exposure to the Ir-Cp^{xph} compounds at equipotent IC_{50} concentrations. B) Cellular accumulation of Ir after 4 h of exposure to the Ir-Cp^{xph} compounds at equipotent IC_{50} concentrations at 4°C and 37°C.

Conclusions

We report the synthesis of novel cyclic peptide-polymer conjugates able to carry organoiridium anticancer complexes. 2-Hydroxypropyl methacrylamide (HPMA) was copolymerized with a novel pyridine-containing monomer which provides a specific binding site for the complexation of highly potent candidate anticancer complexes [(Cp*)Ir(phpy)Cl] and [(Cp^{xph})Ir(phpy)Cl]. The copolymer was then conjugated to self-assembling cyclic peptides using HBTU coupling. The self-assembly of these conjugates was studied by static light scattering and small angle neutron scattering, which revealed that the building blocks form short cylinders about 20 nm in length on average. These drug-bearing nanotubes exhibited comparable or increased toxicity towards human ovarian cancer cells compared to the free drug. Remarkably, their toxicity towards a healthy cell model was lower than the free drug, suggesting a degree of selectivity towards cancer cells. Interestingly, the nanotubes also showed higher toxicity towards cancer cells when compared to the drug-bearing polymers used as a non-assembling control and more conventional example of a drug delivery vector. The analysis of the amount of iridium accumulated in the cells after equipotent and equimolar uptakes revealed that a similar percentage of iridium enters the cells in each case, indicating that the drug-bearing conjugates

do not enhance the iridium uptake, but rather exhibit a more efficient mode of action. Investigations of the mechanisms of entry and partitioning profile of the drug into different organelles revealed that energy-dependent mechanisms of cell uptake account for a higher fraction of the accumulated iridium in the case of the polymer and conjugate than for the free drug.

Supporting information

Characterization of monomers and polymers, polymerization kinetics, SANS and SLS analysis, cell viability in presence of drug-free compounds.

Acknowledgements

We thank the Royal Society Wolfson Merit Award (WM130055; S.P.), the Monash-Warwick Alliance (S.C.L.; S.P.; J.S.) and the ARC (DP140100241; K.A.J.; S.P.), CRUK/EPSRC (C53561/A19933; C.S.-C.; P.J.S.; S.P.), ERC (TUSUPO 647106; S.C.; S.P.) for financial support. J.C.B. thanks the German Science Foundation (DFG) for granting a full postdoctoral fellowship (BR 4905/1-1). We thank ISIS for neutron scattering beam time and Dr. Sarah Rodgers for instrument training and support.

Authors contributions

Conceptualization – S.C.L., J.S., P.J.S., K.A.J, S.P.; Methodology – S.C.L, J.C.B., I.R.-C.; Resources – A.H.; Formal Analysis – S.C.L, J.P.C.C., S.C.; Investigation – S.C.L., I.R.-C., C.S.-C, J-I.S.; Writing – Original Draft, S.C.L; Writing – Review & Editing, all authors.

References

(1) Wang, A. Z.; Langer, R.; Farokhzad, O. C., Nanoparticle Delivery of Cancer Drugs. *Annu, Rev. Med.* **2012,** *63* (1), 185-198.

(2) Petros, R. A.; DeSimone, J. M., Strategies in the design of nanoparticles for therapeutic applications. *Nat. Rev. Drug Discovery* **2010,** *9* (8), 615-627.

(3) Lammers, T.; Kiessling, F.; Hennink, W. E.; Storm, G., Drug targeting to tumors: Principles, pitfalls and (pre-) clinical progress. *J. Controlled Release* **2012,** *161* (2), 175-187.

(4) Maeda, H.; Wu, J.; Sawa, T.; Matsumura, Y.; Hori, K., Tumor vascular permeability and the EPR effect in macromolecular therapeutics: a review. *J. Controlled Release* **2000,** *65* (1–2), 271-284.

(5) Nicolas, J.; Mura, S.; Brambilla, D.; Mackiewicz, N.; Couvreur, P., Design, functionalization strategies and biomedical applications of targeted biodegradable/biocompatible polymer-based nanocarriers for drug delivery. *Chem. Soc. Rev.* **2013,** *42* (3), 1147-1235.

(6) Chou, L. Y. T.; Ming, K.; Chan, W. C. W., Strategies for the intracellular delivery of nanoparticles. *Chem. Soc. Rev.* **2011,** *40* (1), 233-245.

(7) Ghadiri, M. R.; Granja, J. R.; Milligan, R. A.; McRee, D. E.; Khazanovich, N., Self-assembling organic nanotubes based on a cyclic peptide architecture. *Nature* **1993,** *366* (6453), 324-327.

(8) Chapman, R.; Danial, M.; Koh, M. L.; Jolliffe, K. A.; Perrier, S., Design and properties of functional nanotubes from the self-assembly of cyclic peptide templates. *Chem. Soc. Rev.* **2012,** *41* (18), 6023-6041.

(9) Geng, Y.; Dalhaimer, P.; Cai, S. S.; Tsai, R.; Tewari, M.; Minko, T.; Discher, D. E., Shape effects of filaments versus spherical particles in flow and drug delivery. *Nat. Nanotechnol.* **2007,** *2* (4), 249-255.

(10) Truong, N. P.; Quinn, J. F.; Whittaker, M. R.; Davis, T. P., Polymeric filomicelles and nanoworms: two decades of synthesis and application. *Polym. Chem.* **2016,** *7* (26), 4295-4312.

(11) Muraoka, T.; Koh, C. Y.; Cui, H. G.; Stupp, S. I., Light-Triggered Bioactivity in Three Dimensions. *Angew. Chem. Int. Ed.* **2009,** *48* (32), 5946-5949.

(12) Mandal, S.; Eksteen-Akeroyd, Z. H.; Jacobs, M. J.; Hammink, R.; Koepf, M.; Lambeck, A. J. A.; van Hest, J. C. M.; Wilson, C. J.; Blank, K.; Figdor, C. G.; Rowan, A. E., Therapeutic nanoworms: towards novel synthetic dendritic cells for immunotherapy. *Chem. Sci.* **2013,** *4* (11), 4168-4174.

(13) Kumar, S.; Anselmo, A. C.; Banerjee, A.; Zakrewsky, M.; Mitragotri, S., Shape and size-dependent immune response to antigen-carrying nanoparticles. *J. Controlled Release* **2015,** *220, Part A*, 141-148.

(14) Blunden, B. M.; Chapman, R.; Danial, M.; Lu, H. X.; Jolliffe, K. A.; Perrier, S.; Stenzel, M. H., Drug Conjugation to Cyclic Peptide-Polymer Self-Assembling Nanotubes. *Chem. Eur. J.* **2014,** *20* (40), 12745-12749.

(15) Wang, Y.; Yi, S.; Sun, L.; Huang, Y.; Lenaghan, S. C.; Zhang, M., Doxorubicin-Loaded Cyclic Peptide Nanotube Bundles Overcome Chemoresistance in Breast Cancer Cells. *J. Biomed. Nanotechnol.* **2014,** *10* (3), 445-454.

(16) Chen, J.; Zhang, B.; Xia, F.; Xie, Y.; Jiang, S.; Su, R.; Lu, Y.; Wu, W., Transmembrane delivery of anticancer drugs through self-assembly of cyclic peptide nanotubes. *Nanoscale* **2016,** *8* (13), 7127-7136.

(17) Strohalm, J.; Kopeček, J., Poly[N-(2-hydroxypropyl)methacrylamide]. IV. Heterogeneous polymerization. *Angew. Makromol. Chem.* **1978,** *70* (1), 109-118.

(18) Kopeček, J.; Kopečková, P., HPMA copolymers: Origins, early developments, present, and future. *Adv. Drug Delivery Rev.* **2010,** *62* (2), 122-149.

(19) Sanchis, J.; Canal, F.; Lucas, R.; Vicent, M. J., Polymer-drug conjugates for novel molecular targets. *Nanomedicine* **2010,** *5* (6), 915-935.

(20) Duncan, R., Polymer conjugates as anticancer nanomedicines. *Nat. Rev. Cancer* **2006,** *6* (9), 688-701.

(21) Liu, Z.; Romero-Canelon, I.; Qamar, B.; Hearn, J. M.; Habtemariam, A.; Barry, N. P. E.; Pizarro, A. M.; Clarkson, G. J.; Sadler, P. J., The Potent Oxidant Anticancer Activity of Organoiridium Catalysts. *Angew. Chem. Int. Ed.* **2014,** *53* (15), 3941-3946.

(22) Liu, Z.; Sadler, P. J., Organoiridium Complexes: Anticancer Agents and Catalysts. *Acc. Chem. Res.* **2014,** *47* (4), 1174-1185.

(23) Larnaudie, S. C.; Brendel, J. C.; Jolliffe, K. A.; Perrier, S., Cyclic peptide–polymer conjugates: Grafting-to vs grafting-from. *J. Polym. Sci., Part A: Polym. Chem.* **2016,** *54* (7), 1003-1011.

(24) Catrouillet, S.; Brendel, J. C.; Larnaudie, S.; Barlow, T.; Jolliffe, K. A.; Perrier, S., Tunable Length of Cyclic Peptide–Polymer Conjugate Self-Assemblies in Water. *ACS Macro Letters* **2016,** *5* (10), 1119-1123.

(25) Liu, Z.; Habtemariam, A.; Pizarro, A. M.; Clarkson, G. J.; Sadler, P. J., Organometallic Iridium(III) Cyclopentadienyl Anticancer Complexes Containing C,N-Chelating Ligands. *Organometallics* **2011,** *30* (17), 4702-4710.

(26) Liu, Z.; Salassa, L.; Habtemariam, A.; Pizarro, A. M.; Clarkson, G. J.; Sadler, P. J., Contrasting Reactivity and Cancer Cell Cytotoxicity of Isoelectronic Organometallic Iridium(III) Complexes. *Inorg. Chem.* **2011,** *50* (12), 5777-5783.

(27) http://www.isis.stfc.ac.uk.

(28) Heenan, R. K.; Rogers, S. E.; Turner, D.; Terry, A. E.; Treadgold, J.; King, S. M., Small Angle Neutron Scattering Using Sans2d. *Neutron News* **2011,** *22* (2), 19-21.

(29) http://www.mantidproject.org.

(30) Wignall, G. D.; Bates, F. S., Absolute calibration of small angle neutron scattering data. *J. Appl. Crystallogr.* **1987,** *20*, 28-40.

(31) Liu, Z.; Romero-Canelón, I.; Habtemariam, A.; Clarkson, G. J.; Sadler, P. J., Potent Half-Sandwich Iridium(III) Anticancer Complexes Containing C^N-Chelated and Pyridine Ligands. *Organometallics* **2014,** *33* (19), 5324-5333.

(32) Scales, C. W.; Vasilieva, Y. A.; Convertine, A. J.; Lowe, A. B.; McCormick, C. L., Direct, Controlled Synthesis of the Nonimmunogenic, Hydrophilic Polymer, Poly(N-(2-hydroxypropyl)methacrylamide) via RAFT in Aqueous Media. *Biomacromolecules* **2005,** *6* (4), 1846-1850.

(33) Hong, C.-Y.; Pan, C.-Y., Direct Synthesis of Biotinylated Stimuli-Responsive Polymer and Diblock Copolymer by RAFT Polymerization Using Biotinylated Trithiocarbonate as RAFT Agent. *Macromolecules* **2006,** *39* (10), 3517-3524.

(34) Pedersen, J. S., Form factors of block copolymer micelles with spherical, ellipsoidal and cylindrical cores. *J. Appl. Crystallogr.* **2000,** *33* (1), 637-640.

(35) Chapman, R.; Koh, M. L.; Warr, G. G.; Jolliffe, K. A.; Perrier, S., Structure elucidation and control of cyclic peptide-derived nanotube assemblies in solution. *Chem. Sci.* **2013,** *4* (6), 2581-2589.

(36) Liu, Z.; Habtemariam, A.; Pizarro, A. M.; Fletcher, S. A.; Kisova, A.; Vrana, O.; Salassa, L.; Bruijnincx, P. C. A.; Clarkson, G. J.; Brabec, V.; Sadler, P. J., Organometallic Half-Sandwich Iridium Anticancer Complexes. *J. Med. Chem.* **2011,** *54* (8), 3011-3026.

(37) van Rijt, S. H.; Romero-Canelon, I.; Fu, Y.; Shnyder, S. D.; Sadler, P. J., Potent organometallic osmium compounds induce mitochondria-mediated apoptosis and S-phase cell cycle arrest in A549 non-small cell lung cancer cells. *Metallomics* **2014,** *6* (5), 1014-1022.

(38) Novohradsky, V.; Liu, Z.; Vojtiskova, M.; Sadler, P. J.; Brabec, V.; Kasparkova, J., Mechanism of cellular accumulation of an iridium(III) pentamethylcyclopentadienyl anticancer complex containing a C,N-chelating ligand. *Metallomics* **2014,** *6* (3), 682-690.

(39) Puckett, C. A.; Ernst, R. J.; Barton, J. K., Exploring the cellular accumulation of metal complexes. *Dalton Transactions* **2010,** *39* (5), 1159-1170.

TOC

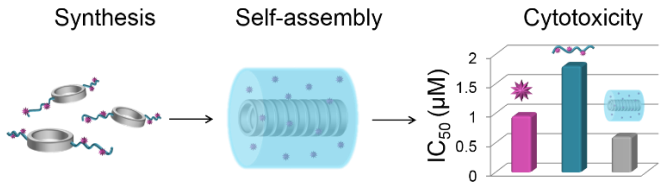

Title: Cyclic peptide-polymer nanotubes as efficient and highly potent drug delivery systems for organometallic anticancer complexes

Authors: Sophie C. Larnaudie, Johannes C. Brendel, Isolda Romero-Canelón, Carlos Sanchez-Cano, Sylvain Catrouillet, Joaquin Sanchis, James P. C. Coverdale, Ji-Inn Song, Abraha Habtemariam, Peter J. Sadler, Katrina A. Jolliffe, and Sébastien Perrier